ORIGINAL ARTICLE

Downregulation of circATXN7 represses non-small cell lung cancer growth by releasing miR-7-5p

Dongliang Li | Zejun Fu | Chaoqun Dong | Yongming Song

Department of Thoracic Surgery, Shanxi Province Cancer Hospital, Shanxi Hospital Affiliated to Cancer Hospital, Chinese Academy of Medical Sciences, Cancer Hospital Affiliated to Shanxi Medical University, Taiyuan, Shanxi, China

Correspondence
Yongming Song, No. 1 Department of Thoracic Surgery, Shanxi Province Cancer Hospital, Shanxi Hospital Affiliated to Cancer Hospital, Chinese Academy of Medical Sciences, Cancer Hospital Affiliated to Shanxi Medical University, No. 3 Workers New Street, Taiyuan City, Shanxi Province, 030000, PR China.
Email: songyongming0303@163.com

Abstract

Background: Circular RNAs (circRNAs) participate in the occurrence and progression of many cancers. CircRNA ataxin 7 (circATXN7) (circBase ID: hsa_circ_0066436) plays a promoting influence on gastric cancer progression. However, the biological role of circATXN7 in non-small cell lung cancer (NSCLC) is indistinct.

Methods: Levels of circATXN7, microRNA (miR)-7-5p, and profilin 2 (PFN2) mRNA were detected using quantitative real-time polymerase chain reaction (RT-qPCR). Proliferation, apoptosis, metastasis, and invasion were analyzed using cell counting kit-8 (CCK-8), colony formation, 5-ethynyl-2′-deoxyuridine (EdU), flow cytometry, and transwell assays. Protein levels were analyzed using western blotting (WB) and immunohistochemistry (IHC). The relationship between circATXN7 or PFN2 and miR-7-5p was analyzed by dual-luciferase reporter and RNA immunoprecipitation (RIP) assays. The biological function of circATXN7 was verified by xenograft assay.

Results: CircATXN7 and PFN2 were highly expressed in NSCLC, whereas miR-7-5p expression had the opposite trend. CircATXN7 overexpression constrained apoptosis and promoted proliferation, metastasis, invasion, and epithelial-mesenchymal transition of NSCLC cells, but circATXN7 silencing played the opposing influence and repressed xenograft tumor growth in vivo. CircATXN7 served as a miR-7-5p sponge, and circATXN7 regulated malignant behaviors of NSCLC cells through sponging miR-7-5p. PFN2 acted as a miR-7-5p target. PFN2 silencing overturned the promoting effect of miR-7-5p inhibitor on NSCLC cell malignancy, while PFN2 overexpression reversed the inhibitory impact of miR-7-5p mimic on NSCLC cell malignancy.

Conclusion: CircATXN7 accelerated the malignancy of NSCLC cells through adsorbing miR-7-5p and upregulating PFN2, offering evidence to support circATXN7 as a target for NSCLC treatment.

KEYWORDS
circATXN7, miR-7-5p, NSCLC, PFN2

INTRODUCTION

Lung cancer (LC) is a malignant tumor originating from the bronchial mucosa or glands of the lungs.[1] The occurrence of LC is related to family history, smoking, chronic inflammation of the lungs, tuberculosis, environmental pollution, and occupational exposure.[2] Non-small cell lung cancer (NSCLC) accounts for up to 85% of all LC.[3] Many NSCLC patients are already in the advanced stage when they are diagnosed.[4] Currently, the mechanism of NSCLC progression has not been fully elucidated. Therefore, exploring the mechanisms related to NSCLC progression is conducive to the development of new treatment strategies.

Circular RNAs (circRNAs) are a novel class of RNA transcripts that have closed-loop structures generated by back-splicing.[5] Also, the special structure of circRNAs

protects them from degradation by RNA exonuclease or RNase R, which makes them more promising as diagnostic markers and therapeutic targets for diseases than linear RNAs.[6] Most circRNAs show cell type- or tissue-specific expression and are the main regulators of gene expression and cell function.[7] Emerging evidence has uncovered that circRNAs actively participate in tumor growth, including NSCLC.[8] For instance, circRNA DCUN1D4 plays a suppressive influence on lung adenocarcinoma cell glycolysis and metastasis through stabilizing TXNIP expression.[9] CircRNA ACGAP1 exerts a promoting effect on cell proliferation by upregulating CDKL1 in NSCLC.[10] CircRNA hsa_circ-ATXN7_010 (circATXN7) (circBase ID: hsa_circ_0066436) is derived from the ataxin 7 (ATXN7) gene (exons 9–11) located on chr3: 63973734–63 976 535. Also, circATXN7 has been reported to promote gastric cancer progression by elevating ENTPD4 expression.[11] However, the regulation mechanism of circATXN7 in NSCLC is indistinct.

A considerable number of reports have proved that circRNAs are related to the progression of some diseases by functioning as microRNA (miR) sponges.[12] MiRs, small single-stranded non-coding RNA molecules, exert a pivotal role in post-transcriptional gene regulation by means of mRNA degradation or translational repression.[13] Functional studies have confirmed that miRs dysregulation is the cause of many cancers.[14] MiR-7-5p has been found to exert an anticancer effect or promoting effect in different types of cancer. MiR-7-5p has also been reported to function as a tumor repressor in glioma,[15] nasopharyngeal cancer,[16] and LC,[17,18] while miR-7-5p exerts an oncogenic role in cervical cancer.[19] Also, miR-7-5p has been found to play an antitumor activity in NSCLC via targeting NVOA2.[20] At present, the mechanism related to the imbalance of miR-7-5p in NSCLC has not been fully explained.

Profilin 2 (PFN2) is an actin-binding protein that participates in cell shape changes and cell movement by regulating the reorganization of the actin cytoskeleton and actin polymerization.[21] Previously, PFN2 was considered to only be involved in the development of the nervous system.[22] Recently, PFN2 has been exposed as an oncogene in breast,[23] head and neck cancers,[24] and NSCLC.[25] Currently, the mechanism that regulates the abnormal expression of PFN2 in NSCLC is still unclear.

Herein, we verified that circATXN7 plays a promoting influence on the malignant behavior of NSCLC cells. Importantly, circATXN7 functions as a miR-7-5p decoy and elevates PFN2 expression by adsorbing miR-7-5p, resulting in accelerating malignant behaviors of NSCLC cells.

METHODS

Clinical specimens

Collection of clinical samples from 34 NSCLC patients was done at Shanxi Province Cancer Hospital, Shanxi Hospital Affiliated to Cancer Hospital, Chinese Academy of Medical Sciences, Cancer Hospital Affiliated to Shanxi Medical University, including NSCLC tissues and adjacent nontumor tissues. Registered patients signed informed consents. The utilization of human clinical specimens followed the procedures authorized by the Ethics Committee of Shanxi Province Cancer Hospital, Shanxi Hospital Affiliated to Cancer Hospital, Chinese Academy of Medical Sciences, Cancer Hospital Affiliated to Shanxi Medical University. Patient information is shown in Table S1.

Cell culture

Human tracheobronchial epithelial cells 16HBE (Procell) and NSCLC cell lines (NCI-H460, NCI-H1299, LK-2, and A549) (Cobioer) were cultured in Roswell Park Memorial Institute-1640 medium (Invitrogen) or Ham's F-12K medium (Invitrogen) supplemented with 10% fetal bovine serum (Invitrogen) and 1% penicillin/streptomycin (Sigma) at 37°C with 5% CO_2.

Oligonucleotides and plasmids

The overexpression plasmids of circATXN7 (circATXN7) were generated with empty pCD5-ciR vectors (Vector) (Geneseed), while the overexpression plasmids of PFN2 (PFN2) were produced with empty pcDNA vectors (Invitrogen). The oligonucleotide sequences were synthesized by AoKe Biotech, including short hairpin (sh) RNA against circATXN7 (sh-circATXN7), negative control for sh-circATXN7 (sh-NC), small interference (si) RNA targeting PFN2 (si-PFN2), negative control for si-PFN2 (si-con), miR-7-5p inhibitor (in-miR-7-5p), negative control for miR inhibitor (in-miR-NC), miR-7-5p mimic (miR-7-5p), and negative control for miR mimic (miR-NC). Cell transfection was conducted using lipofectamine RNAiMAX (Invitrogen).

Quantitative real-time polymerase chain reaction

The isolation of cytoplasmic RNA and nuclear RNA was carried out using the PARIS kit (Invitrogen). Total RNA was isolated with the TRIzol kit (Invitrogen) and quantified with the NanoDrop 2000c spectrophotometer (Invitrogen). For RNA digestion, total RNA derived from NSCLC cells was treated with RNase R (3 U/μg, BioVision), and diethylpyrocarbonate-treated water (Invitrogen) was utilized as a negative control. Complementary DNA was generated using the SuperScript III (Invitrogen) or miScript II RT Kit (Qiagen), followed by performing qPCR with the SYBR qPCR Master Mix (Roche). All primer sequences are presented in Table 1. Glyceraldehyde-3-phosphate dehydrogenase (GAPDH) and U6 were used as internal references. Relative expression of each gene was figured with the threshold cycle ($2^{-\Delta\Delta Ct}$) method.[26]

T A B L E 1 Primer sequences used for qRT-PCR

Genes	Primer sequences (5′-3′)
circATXN7	Forward (F): 5′-CACAGCTATGGAAACA CATTCCTT-3′
	Reverse (R): 5′-GAGTCCGGATGGCGAATCAA-3′
ATXN7	F: 5′-CAACCTCATGGTGGAGAAGCATC-3′
	R: 5′-ATGTCGGCACAGAGTTTGTCCG-3′
PFN2	F: 5′-TCGGCTACTGCGACGCCAAATA-3′
	R: 5′-GATCACTGAGCATTTCTTCGCGC-3′
GAPDH	F: 5′-GTCTCCTCTGACTTCAACAGCG-3′
	R: 5′-ACCACCCTGTTGCTGTAGCCAA-3′
miR-7-5p	F: 5′-CGCGTGGAAGACTAGTGATTTT-3′
	R: 5′-AGTGCAGGGTCCGAGGTATT-3′
miR-145-5p	F: 5′-CGGTCCAGTTTTCCCAGGA-3′
	R: 5′-AGTGCAGGGTCCGAGGTATT-3′
miR-149-5p	F: 5′-CGTCTGGCTCCGTGTCTTC-3′
	R: 5′-AGTGCAGGGTCCGAGGTATT-3′
miR-421	F: 5′-GCGCGATCAACAGACATTAATT-3′
	R: 5′-AGTGCAGGGTCCGAGGTATT-3′
miR-1270	F: 5′-CGCGCTGGAGATATGGAAGA-3′
	R: 5′-AGTGCAGGGTCCGAGGTATT-3′
miR-1294	F: 5′-GCGTGTGAGGTTGGCATTG-3′
	R: 5′-AGTGCAGGGTCCGAGGTATT-3′
U6	F: 5′-CTCGCTTCGGCAGCACA-3′
	R: 5′-AACGCTTCACGAATTTGCGT-3′

Cell counting kit-8 assay

The transfected NSCLC cells were seeded in 96-well plates (1×10^3). Subsequently, the cell counting kit-8 (CCK-8) reagent (10 μl) (Beyotime) was added at the specified time. The optical density (OD) value was evaluated with the SpectraMax M2 microplate detection system (MD).

Colony formation assay

NSCLC cells (3×10^2) were cultured in 6-well plates for 12 days. Subsequently, the colonies were fixed with 4% paraformaldehyde (Beyotime), followed by staining with 0.5% crystal violet (Beyotime) and counting and capturing with a fluorescent microscope (Olympus).

5-ethynyl-2′-deoxyuridine assay

Cell proliferation was determined by 5-ethynyl-2′-deoxyuridine (EdU) assay with the Cell-Light EdU DNA Cell Proliferation Kit (RiboBio). In brief, the EdU solution (50 mM) was added and then 2 h later, the cells were fixed with 4% paraformaldehyde (Beyotime) and then stained with Apollo Dye Solution and 4′,6-diamidino-2-phenylindole (DAPI).

A fluorescent microscope (Olympus) was utilized to visualize the cells.

Flow cytometry assay

The transfected NSCLC cells were collected and then detached with 0.025% trypsin (Sigma). Cell apoptosis was evaluated with the Annexin V-fluorescein isothiocyanate (FITC)/propidium iodide (PI) apoptosis detection kit (Sigma) based on the manufacturer's instructions. The apoptotic rate was determined using cytoflex flow cytometry (Beckman Coulter).

Transwell assay

Transwell chambers without Matrigel (#3422, Costar) were used for analysis of cell metastasis. In summary, the cells (1×10^5) in 200 μl serum-free cell culture medium were placed on the apical chamber and 600 μl cell culture medium encompassing 10% fetal bovine serum (Sigma) was added to the basolateral chamber. Then, 24 h later, the migrated cells were stained with 0.1% crystal violet (Beyotime) and counted with a microscope (Olympus). Notably, the experimental procedures for cell metastasis and invasion were the same, the only difference was that the invasion experiment was performed with the transwell chamber with Matrigel (#354480, Costar).

Western blotting

Total protein was extracted using the radioimmunoprecipitation buffer (Beyotime). Western blotting (WB) was executed as previously described.[27] Antibodies utilized for WB were as follows: E-cadherin (#PA5-32178, 1:3000, Invitrogen), N-cadherin (#PA5-29570, 1:1000, Invitrogen), vimentin (#10366-1-AP, 1:3000, Invitrogen), PFN2 (#PA5-21959, 1:1000, Invitrogen), GAPDH (#PA1-16777, 1:4000, Invitrogen), NOVA2 (#PA5-69076, 1.25 μg/ml, Invitrogen), Lamin A/C (#MA3-1000, 1:500, Invitrogen), Calreticulin (#MA5-15382, 1:1000, Invitrogen), goat rabbit IgG (#31460, 1:10,000, Invitrogen), and goat anti-mouse IgG (#31430, 1:5000, Invitrogen). The blots were developed using the Pierce ECL WB Substrate (Invitrogen).

Dual-luciferase reporter assay

MiRs that might interact with circATXN7 were jointly predicted using circBank, starBase, and CircInteractome databases. The binding sites between miR-7-5p and PFN2 3′ untranslated region (UTR) were predicted using the TargetScan database. To verify the relationship between circATXN7 or PFN2 and miR-7-5p, the wild-type (WT) sequences of circATXN7 and PFN2 3′UTR and their

mutant (MUT) sequences were inserted into the pMIR-REPORT reporter (Applied Biosystems), respectively. NSCLC cells were transfected with miR-7-5p mimic or miR-NC together with a luciferase reporter. The luciferase activity was assessed using the Pierce Renilla-Firefly Luciferase Dual Assay Kit (Invitrogen).

RNA immunoprecipitation assay

The interaction between circATXN7 or PFN2 and miR-7-5p was verified by RNA immunoprecipitation (RIP) analysis with the Magna RIP kit (Millipore). In brief, NSCLC cells were lysed and then centrifuged at 4°C (14,000 rpm, 10 min). The supernatant was incubated with magnetic beads conjugated to IgG antibody (Abcam) or Ago2 antibody (Abcam). The abundance of circATXN7 or PFN2 and miR-7-5p in immunoprecipitated RNA was assessed by RT-qPCR.

Xenograft assay

Twelve BALB/c nude mice (4–6 weeks old) were purchased from Vital River Laboratory. The execution of animal experiments followed the procedures approved by the Animal Ethics Committee of Shanxi Province Cancer Hospital, Shanxi Hospital Affiliated to Cancer Hospital, Chinese Academy of Medical Sciences, Cancer Hospital Affiliated to Shanxi Medical University. Briefly, A549 cells carrying lentivirus-mediated sh-circATXN7 or sh-NC were subcutaneously injected into the right flank of nude mice ($n = 6$ mice per group). Tumor volume was measured every 4 days from day 7 (volume = [length $\times$ width^2]/2), and then 27 days later, all mice were sacrificed to strip the xenograft tumors and weighed.

Immunohistochemistry

Paraffin-embedded mice tissue sections (5 μm thick) were incubated with anti-PFN2 antibody (#PA5-21959, 1:500, Invitrogen) at 4°C for 12 h. The Vectastain Universal Elite ABC Kit (Vector Laboratories) was used for immunohistochemistry (IHC) staining based on the manufacturer's instructions.

Statistical analysis

At least three repeats were conducted for each experiment. SPSS Statistical software version 17.0 (SPSS) was utilized for statistical analyses. All data are presented as mean ± SD. Student's t-test and analysis of variance were used to compare the differences between two groups or more groups. A value of $p < 0.05$ was considered statistically significant.

RESULTS

CircATXN7 was highly expressed in NSCLC

CircATXN7 (circBase ID: hsa_circ_0066436) contains 587 nucleotides and is produced from the ATXN7 gene (exons 9–11) in chr3: 63973734–63976535 (Figure 1a). To validate the expression trend of circATXN7 in NSCLC, we detected circATXN7 expression in NSCLC tissues and cells. As exhibited in Figure 1b,c, there was observable upregulation of circATXN7 in NSCLC tissues and cells (NCI-H460, NCI-H1299, LK-2, and A549) compared to their matched negative controls. A significant correlation between TNM grade, lymph node metastasis, or tumor size and high circATXN7 level was obtained by Chi-square analysis, as shown in Table S1. To verify the stability of circATXN7, we treated RNA extracted from NCI-H460 and A549 cells with RNase R. RT-qPCR showed that RNase R treatment did not affect the level of circATXN7, whereas linear ATXN7 was significantly degraded (Figure 1d,e). Nuclear mass separation with RT-qPCR revealed that circATXN7 was preferentially localized in the cytoplasm of NCI-H460 and A549 cells, and western blotting confirmed good nucleus/cytoplasm fractionation (Figure 1f). These results uncovered that circATXN7 was preferentially localized in the cytoplasm and might participate in the progression of NSCLC.

CircATXN7 facilitated proliferation and curbed apoptosis of NSCLC cells

Next, we carried out gain/loss-of-function experiments to verify the impacts of circATXN7 on NSCLC cell proliferation and apoptosis. RT-qPCR displayed that circATXN7 expression was increased in NCI-H460 cells after circATXN7 transfection and decreased in A549 cells after sh-circATXN7 transfection (Figure 2a,b). CCK-8 and colony formation assays exhibited that circATXN7 overexpression promoted NCI-H460 cell growth and colony formation, whereas circATXN7 knockdown repressed A549 cell growth and colony formation (Figure 2c–f). EdU assay showed that the number of positive cells was elevated in NCI-H460 cells with overexpression of circATXN7 and reduced in A549 cells with knockdown of circATXN7 (Figure 2g–j). Flow cytometry assay revealed that the transfection of circATXN7 repressed the apoptosis of NCI-H460 cells, but the transfection of sh-circATXN7 elevated the apoptosis of A549 cells (Figure 2k,l). Collectively, these findings manifested that circATXN7 accelerated cell proliferation and constrained cell apoptosis in NSCLC cells.

CircATXN7 promoted metastasis, invasion, and epithelial-mesenchymal transition of NSCLC cells

Subsequently, the influence of circATXN7 on NSCLC cell metastasis, invasion, and epithelial-mesenchymal transition
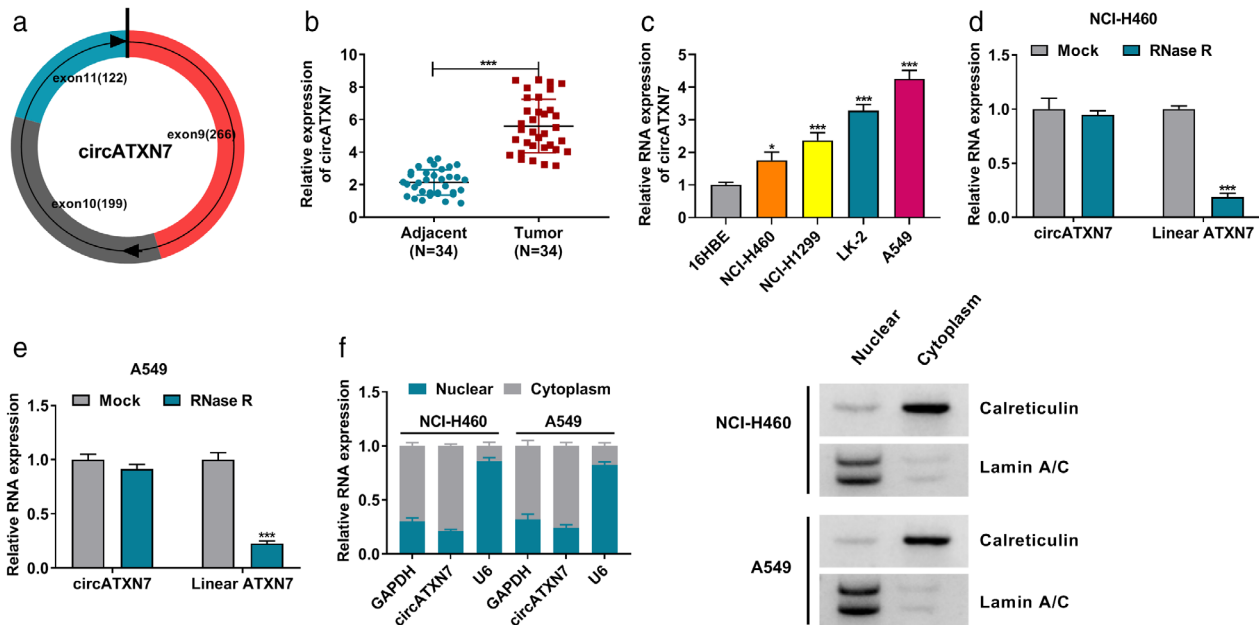
FIGURE 1 CircATXN7 was upregulated in NSCLC. (a) The schematic diagram exhibited the formation of circATXN7. (b and c) RT-qPCR revealed circATXN7 expression in NSCLC tissues and cells, and adjacent nontumor tissues and 16HBE cells were used as negative controls. (d and e) RT-qPCR detected the levels of circATXN7 and linear ATXN7 in RNA extracted from NCI-H460 and A549 cells under RNase R treatment. (f) Nuclear mass separation with RT-qPCR revealed the distribution of circATXN7 in NCI-H460 and A549 cells. Western blotting confirmed good nucleus/cytoplasm fractionation. $^*p < 0.05$ and $^{***}p < 0.001$

(EMT) was surveyed. Transwell assay revealed that the number of metastasizing and invading cells was elevated in -circATXN7-transfected NCI-H460 cells and reduced in sh-circATXN7-transfected A549 cells (Figure 3a,d). Also, circATXN7 upregulation reduced E-cadherin protein level and elevated N-cadherin and vimentin protein levels in NCI-H460 cells, but circATXN7 knockdown elevated E-cadherin protein level and decreased N-cadherin and vimentin protein levels in A549 cells (Figure 3e,f). Together, these results indicated that circATXN7 accelerated NSCLC cell metastasis, invasion, and EMT.

CircATXN7 was identified as a miR-7-5p decoy

Since circATXN7 was mainly located in the cytoplasm, we speculated that circATXN7 might function as a decoy for miRs. Bioinformatic analysis (circBank, starBase, and CircInteractome) exhibited that 6 miRs (miR-7-5p, miR-145-5p, miR-149-5p, miR-421, miR-1270, and miR-1294) might interact with circATXN7 (Figure 4a). RT-qPCR showed that miR-7-5p, miR-145-5p, and miR-149-5p were downregulated in 6 random NSCLC tissues, while miR-421 and miR-1270 were upregulated (Figure 4b). Also, miR-7-5p and miR-145-5p expression were decreased in circATXN7-overexpressed NCI-H460 cells and elevated in circATXN7-suppressed A549 cells, especially the expression of miR-7-5p (Figure 4c,d). The putative binding sites of circATXN7 in miR-7-5p are shown in Figure 4e. Furthermore, the luciferase activity of the circATXN7 WT reporter

was suppressed in miR-7-5p-overexpressed NCI-H460 and A549 cells (Figure 4f,g). The abundance of miR-7-5p and circATXN7 was significantly increased in the immunoprecipitates pulled down by the Ago2 antibody (Figure 4h,i). As expected, miR-7-5p expression was decreased in NSCLC tissues and was negatively correlated with circATXN7 (Figure 4j,k). In addition, miR-7-5p was overtly downregulated in NCI-H460 and A549 cells (Figure 4l). Collectively, these findings suggested that circATXN7 acted as a miR-7-5p sponge in NSCLC cells.

CircATXN7 regulated NSCLC cell malignancy by sponging miR-7-5p

Based on circATXN7 served as a miR-7-5p sponge, we wondered whether circATXN7 regulated NSCLC cell malignancy by sponging miR-7-5p. The overexpression efficiency of miR-7-5p in NCI-H460 cells and the knockdown efficiency of in-miR-7-5p in A549 cells were presented in Figure 5a,b. Moreover, the promotion of proliferation and the repression of apoptosis of NCI-H460 cells caused by circATXN7 upregulation were overturned by miR-7-5p overexpression. However, the silence of miR-7-5p reversed the repression of proliferation and the promotion of apoptosis of A549 cells mediated by circATXN7 knockdown (Figure 5c–j). Also, miR-7-5p elevation offset the promoting impact of circATXN7 overexpression on NCI-H460 cell metastasis and invasion, whereas miR-7-5p inhibitor counteracted the inhibitory influence of circATXN7
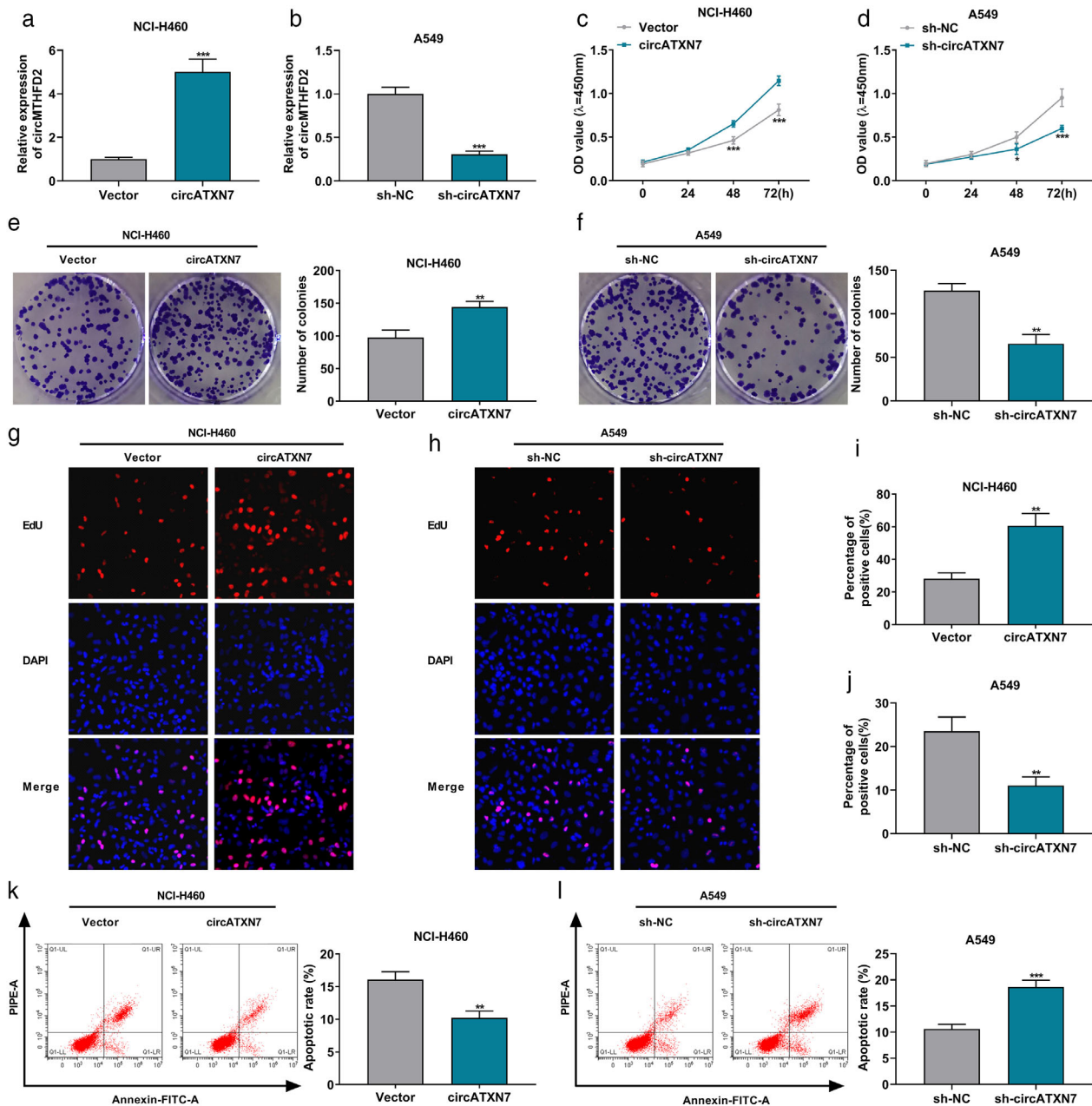
FIGURE 2 CircATXN7 accelerated NSCLC cell proliferation and repressed NSCLC cell apoptosis. (a and b) The overexpression efficiency of circATXN7 in NCI-H460 cells and the knockdown efficiency of sh-circATXN7 in A549 cells were verified by RT-qPCR. (c–j) The proliferation of NCI-H460 cells with upregulation of circATXN7 and A549 cells with inhibition of circATXN7 was analyzed by CCK-8, colony formation, and EdU assays. (k and l) The apoptosis of NCI-H460 cells transfected with circATXN7 and A549 cells transfected with sh-circATXN7 was analyzed by flow cytometry assay. $*p < 0.05$, $**p < 0.01$, and $***p < 0.001$

silencing on A549 cell metastasis and invasion (Figure 5k–n). Furthermore, the protein trends of E-cadherin, N-cadherin, and vimentin in NCI-H460 cells transfected with circATXN7 were overturned by miR-7-5p overexpression, while the protein trends of E-cadherin, N-cadherin, and vimentin in A549 cells mediated by circATXN7 inhibition were restored after miR-7-5p knockdown (Figure 5o,p). These results indicated that circATXN7 promoted NSCLC cell malignancy by sponging miR-7-5p.

PFN2 served as a miR-7-5p target

To further explore the regulation mechanism of circATXN7 in NSCLC, we sought the targets of miR-7-5p. Through bioinformatic analysis (TargetScan database), we discovered that PFN2 might be a miR-7-5p target (Figure 6a). Moreover, the level of PFN2 protein was decreased in miR-7-5p-overexpressed NCI-H460 cells and elevated in miR-7-5p-inhibited A549 cells (Figure 6b,c). Also, miR-7-5p
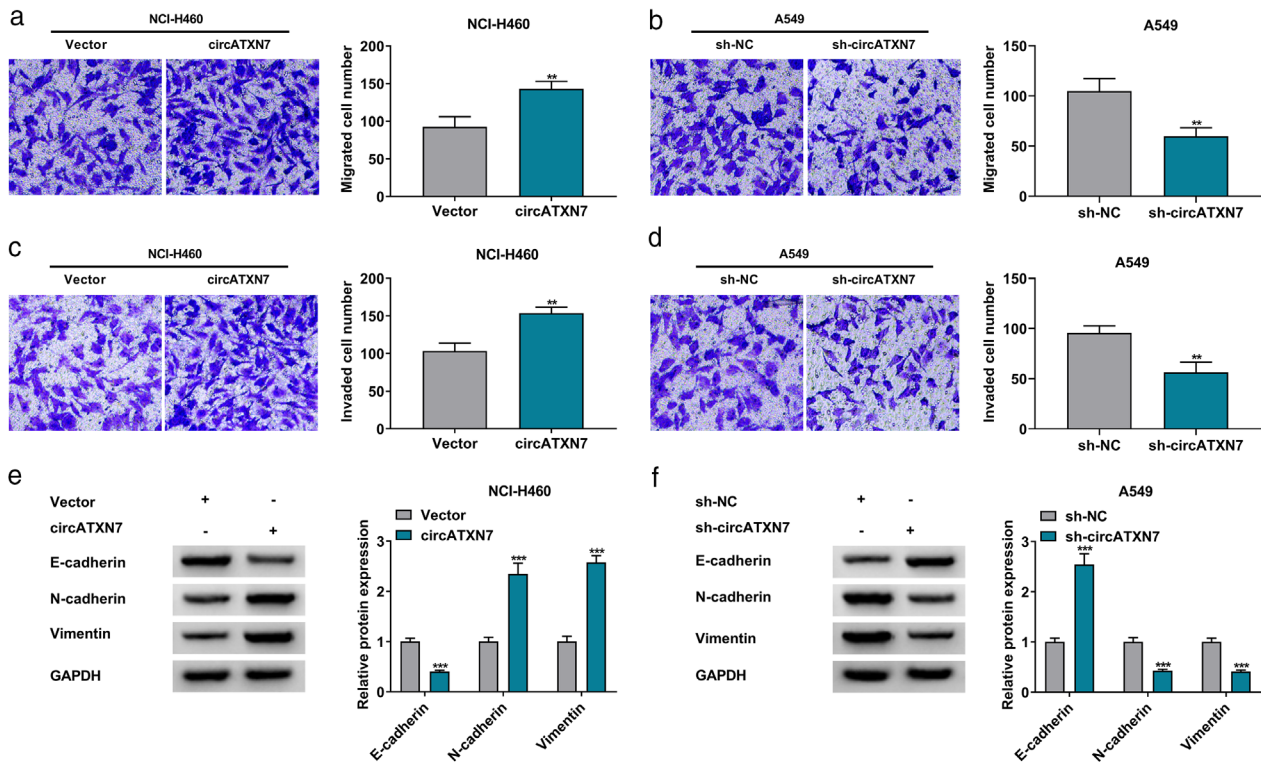
FIGURE 3 CircATXN7 accelerated NSCLC cell metastasis, invasion, and EMT. (a–d) Transwell assay revealed the metastasis and invasion abilities of NCI-H460 cells with upregulation of circATXN7 and A549 cells with inhibition of circATXN7. (e and f) WB detected protein levels of E-cadherin, N-cadherin, and vimentin in NCI-H460 cells transfected with circATXN7 and A549 cells transfected with sh-circATXN7. **$p < 0.01$ and ***$p < 0.001$

overexpression decreased the luciferase activity of the PFN2 3′UTR WT reporter in NCI-H460 and A549 cells (Figure 6d, e). There was a prominent enrichment of PFN2 and miR-7-5p in the immunoprecipitates pulled down by the Ago2 antibody (Figure 6f,g). As expected, the levels of PFN2 mRNA and protein were upregulated in NSCLC tissues (Figure 6h,i). The expression of PFN2 mRNA was also negatively correlated with miR-7-5p and positively correlated with circATXN7 in NSCLC tissues (Figure 6j,k). In addition, the levels of PFN2 mRNA and protein were also elevated in NCI-H460 and A549 cells (Figure 6l,m). Furthermore, the level of PFN2 protein was elevated in circATXN7-transfected NCI-H460 cells and reduced in sh-circATXN7-transfected A549 cells, but these tendencies were restored after miR-7-5p overexpression or silencing (Figure 6n,o). Together, these results suggested that PFN2 was a downstream target of miR-7-5p.

MiR-7-5p repressed NSCLC cell malignancy by targeting PFN2

Because miR-7-5p targeted PFN2, we further explored whether miR-7-5p regulated malignant behaviors of NSCLC cells by targeting PFN2. The knockdown efficiencies of si-PFN2 and in-miR-7-5p in NCI-H460 cells and the overexpression efficiencies of PFN2 and miR-7-5p in A549 cells are shown in Figure 7a,b. Moreover, miR-7-5p inhibition facilitated NCI-H460 cell proliferation and constrained

NCI-H460 cell apoptosis, but these impacts were restored after si-PFN2 introduction. However, miR-7-5p elevation curbed A549 cell proliferation and accelerated A549 cell apoptosis, whereas these trends were reversed after PFN2 overexpression (Figure 7c–j). Furthermore, PFN2 silencing counteracted the promoting effect of miR-7-5p inhibitor on NCI-H460 cell metastasis and invasion, while PFN2 upregulation offset the suppressive influence of miR-7-5p mimic on A549 cell metastasis and invasion (Figure 7K–n). As expected, miR-7-5p inhibitor reduced E-cadherin protein level and elevated N-cadherin and vimentin protein levels in NCI-H460 cells, but these trends were overturned by PFN2 knockdown (Figure 7o). Additionally, miR-7-5p mimic elevated E-cadherin protein level and decreased N-cadherin and vimentin protein levels in A549 cells, whereas these tendencies were reversed after PFN2 upregulation (Figure 7p). These results manifested that miR-7-5p repressed cell malignancy by targeting PFN2 in NSCLC cells.

CircATXN7 knockdown repressed tumor growth in vivo

To verify the influence of circATXN7 knockdown in tumor growth in vivo, A549 cells stably transfected with sh-circATXN7 or sh-NC were injected into nude mice. The results revealed that tumor volume and weight derived from
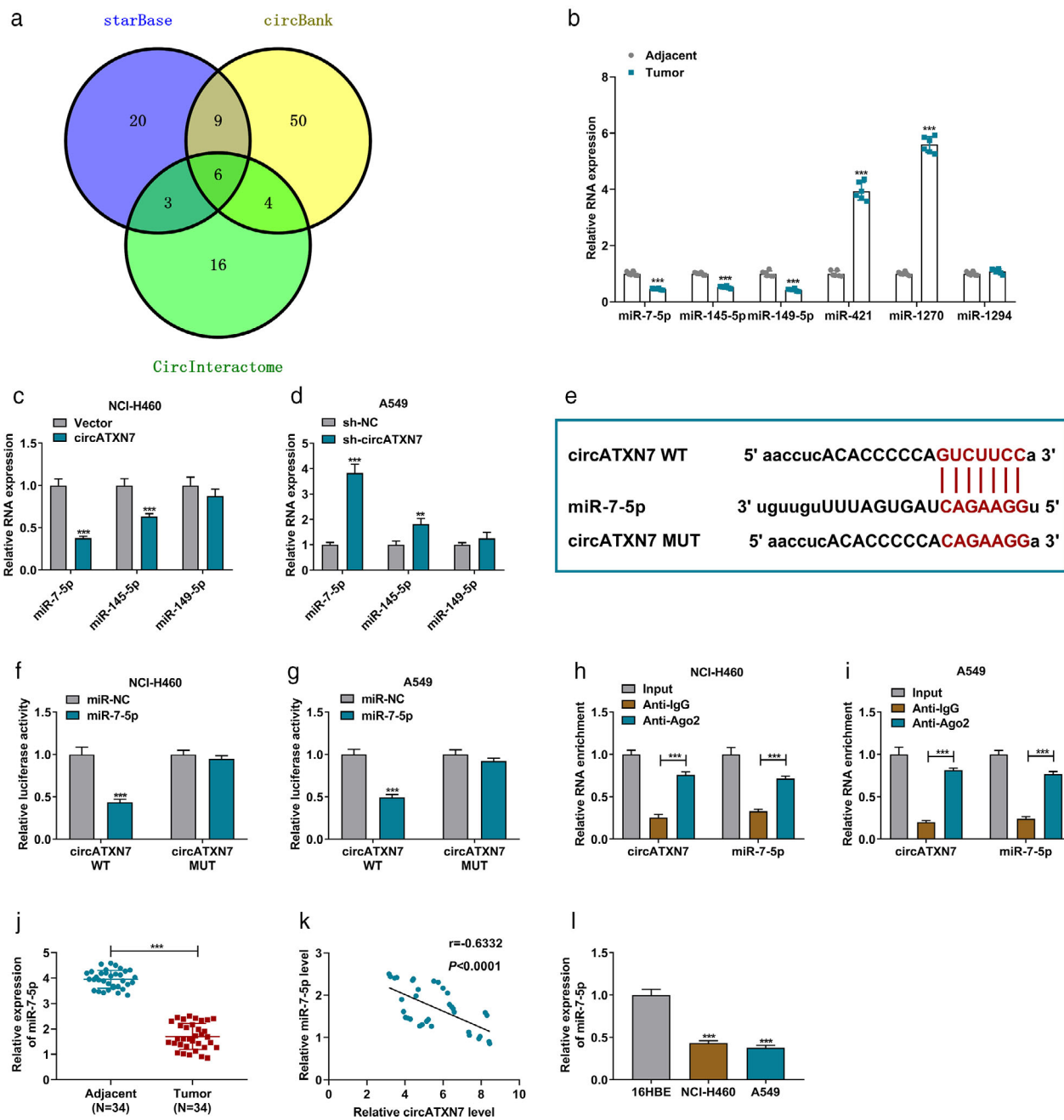
FIGURE 4 CircATXN7 served as a miR-7-5p sponge. (a) The schematic diagram showed the overlapping miRs that might interact with circATXN7 in the circBank, starBase, and CircInteractome databases. (b) RT-qPCR detected the expression of six predicted miRs in six random NSCLC tissues and paired adjacent nontumor tissues. (c and d) RT-qPCR analyzed the expression of miR-7-5p, miR-145-5p, miR-149-5p in circATXN7-overexpressed NCI-H460 cells and circATXN7-suppressed A549 cells. (e) The schematic diagram presented the binding sites between circATXN7 and miR-7-5p. (f–i) The relationship between circATXN7 and miR-7-5p was validated by dual-luciferase reporter and RIP assays. (j) RT-qPCR verified the expression of miR-7-5p in 34 paired NSCLC tissues and adjacent nontumor tissues. (k) Pearson's correlation analysis revealed the correlation between circATXN7 and miR-7-5p in NSCLC tissues. (l) The expression trend of miR-7-5p in NCI-H460 and A549 cells was verified by RT-qPCR. **$p < 0.01$ and ***$p < 0.001$

nude mice injected with A549 cells carrying sh-circATXN7 were smaller and lighter compared to the control group (Figure 8a–c). RT-qPCR exhibited that circATXN7 and PFN2 mRNA were downregulated in mice tumors in the sh-circATXN7 group in contrast to the control group, while miR-7-5p expression had the opposite trend (Figure 8d). WB and IHC analysis showed that the level of PFN2 protein

was also downregulated in mice tumors in the sh-circATXN7 group (Figure 8e,f). In addition, the level of E-cadherin was upregulated in mice tumors in the sh-circATXN7 group, but the levels of N-cadherin and vimentin protein were downregulated (Figure 8g). Collectively, these results suggested that circATXN7 knockdown curbed NSCLC growth in vivo.
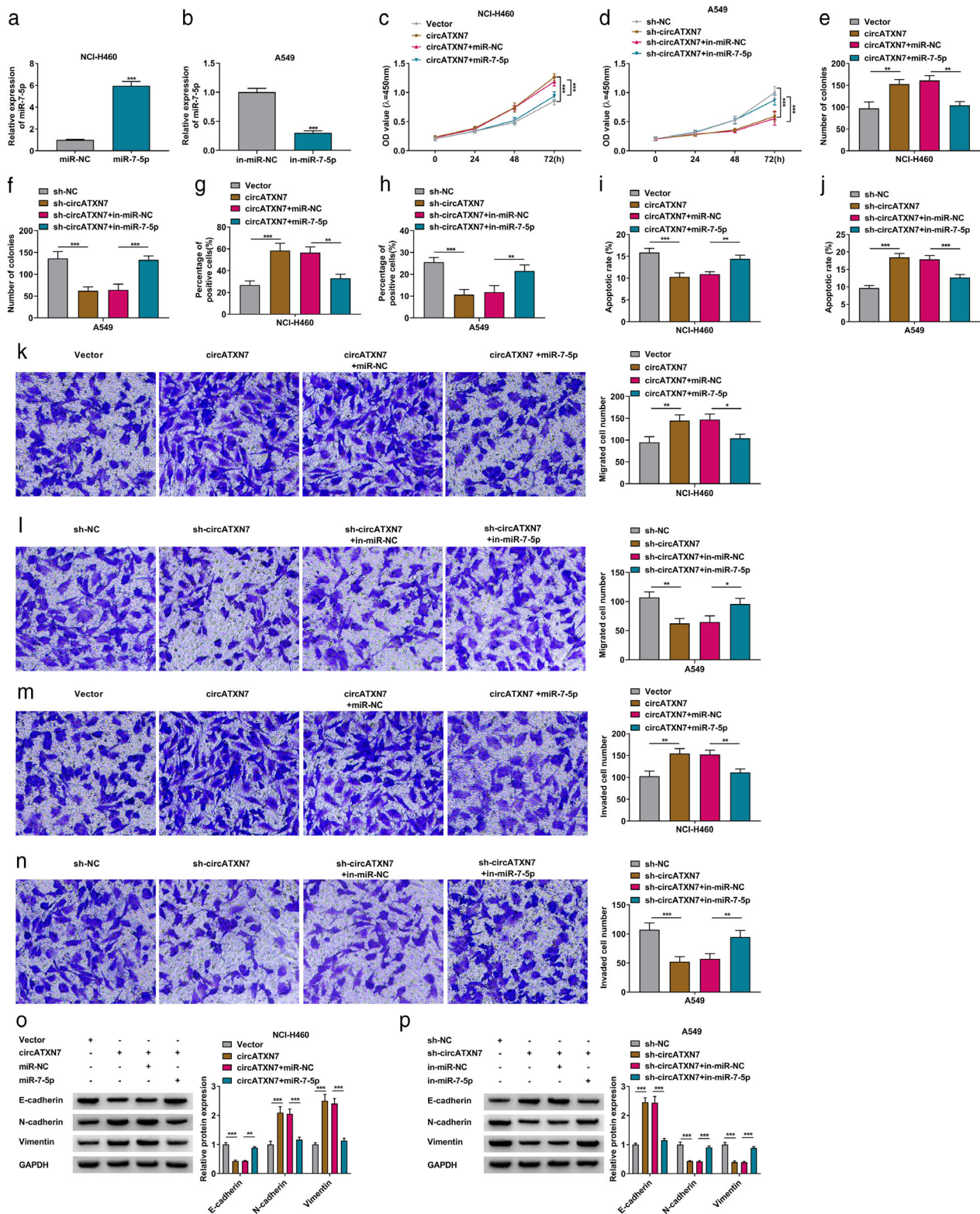
FIGURE 5 CircATXN7 sponged miR-7-5p to regulate NSCLC cell malignancy. (a and b) RT-qPCR verified the overexpression efficiency of miR-7-5p in NCI-H460 cells and the knockdown efficiency of in-miR-7-5p in A549 cells. (c–n) The proliferation, apoptosis, metastasis, and invasion of NCI-H460 cells transfected with vector, circATXN7, circATXN7 + miR-NC, or circATXN7 + miR-7-5p and A549 cells transfected with sh-NC, sh-circATXN7, sh-circATXN7 + in-miR-NC, or sh-circATXN7 + in-miR-7-5p were analyzed by CCK-8, colony formation, EdU, flow cytometry, and transwell assays. (o, p) Protein levels of E-cadherin, N-cadherin, and Vimentin in NCI-H460 cells transfected with vector, circATXN7, circATXN7 + miR-NC, or circATXN7 + miR-7-5p and A549 cells transfected with sh-NC, sh-circATXN7, sh-circATXN7 + in-miR-NC, or sh-circATXN7 + in-miR-7-5p were detected by WB. $*p < 0.05$, $**p < 0.01$, and $***p < 0.001$
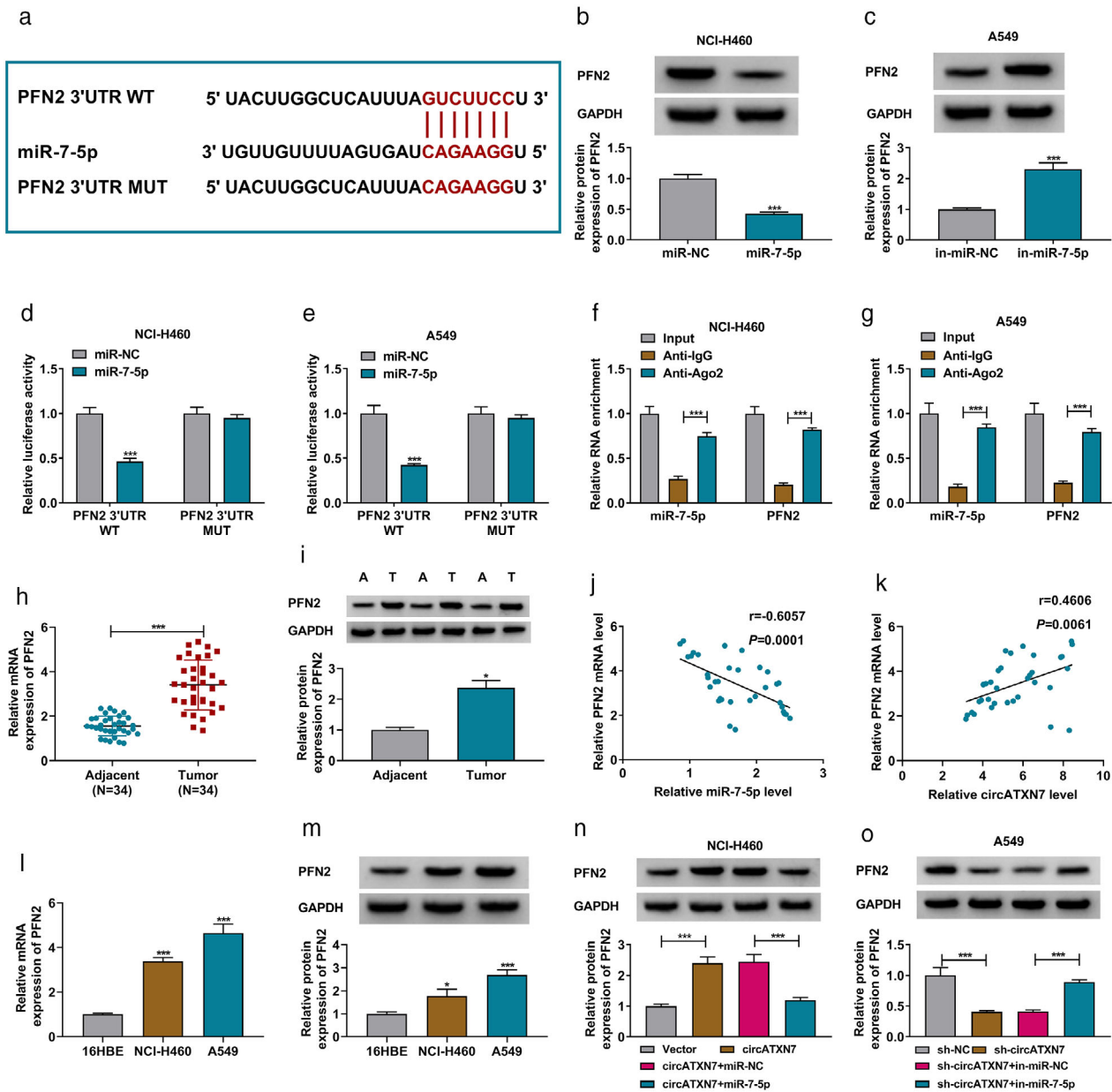
FIGURE 6 PFN2 acted as a target for miR-7-5p. (a) The schematic diagram shows the putative binding sites of PFN2 in miR-7-5p. (b and c) Western blot was used to assess PFN2 protein level in NCI-H460 cells and the elevation of miR-7-5p and A549 cells with an inhibition of miR-7-5p. (d and g) The relationship between PFN2 and miR-7-5p in NCI-H460 and A549 cells was validated by dual-luciferase reporter and RIP assays. (h and i) The levels of PFN2 mRNA and protein in NSCLC tissues were evaluated by RT-qPCR and WB. (j and k) The correlation between PFN2 and miR-7-5p or circATXN7 was analyzed by Pearson's correlation analysis. (l and m) The levels of PFN2 mRNA and protein in NCI-H460 and A549 cells were detected by RT-qPCR and WB. (n and o) Protein level of PFN2 in NCI-H460 cells transfected with vector, circATXN7, circATXN7 + miR-NC, or circATXN7 + miR-7-5p and A549 cells transfected with sh-NC, sh-circATXN7, sh-circATXN7 + in-miR-NC, or sh-circATXN7 + in-miR-7-5p was measured by WB. $*p < 0.05$ and $***p < 0.001$

DISCUSSION

Studies have revealed that differential circRNA expression is observably related to cancer TNM staging, metastasis, and other clinical characteristics of cancer.[28] Also, circRNAs are promising therapeutic targets for cancer, including NSCLC.[29] Herein, we validated that circATXN7 functioned as a miR-7-5p sponge and facilitated NSCLC growth through upregulating PFN2.

It is worth mentioning that our results offer new evidence that circATXN7 facilitates the progression of NSCLC. The inference is based on the following points: (1) circATXN7 was highly expressed in NSCLC; (2) the silence of circATXN7 inhibited NSCLC cell proliferation,
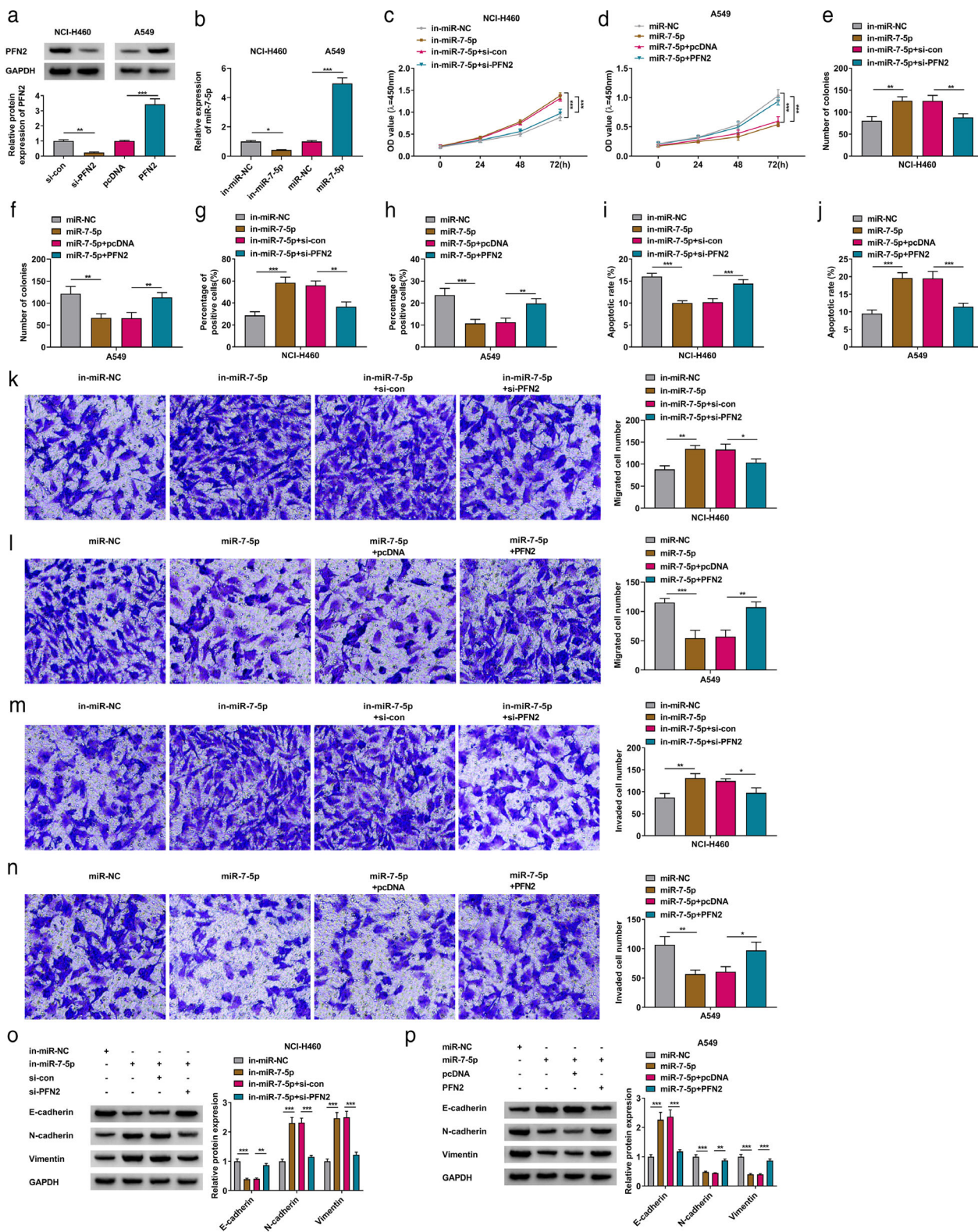
FIGURE 7 MiR-7-5p targeted PFN2 to repress the malignancy of NSCLC cells. (a and b) WB and RT-qPCR validated the knockdown efficiencies of si-PFN2 and in-miR-7-5p in NCI-H460 cells and the overexpression efficiencies of PFN2 and miR-7-5p in A549 cells. (c–n) The proliferation, apoptosis, metastasis, and invasion of NCI-H460 cells transfected with in-miR-NC, in-miR-7-5p, in-miR-7-5p + si-con, or in-miR-7-5p + si-PFN2 and A549 cells transfected with miR-NC, miR-7-5p, miR-7-5p + pcDNA, or miR-7-5p + PFN2 were determined by CCK-8, colony formation, EdU, flow cytometry, and transwell assays. (o and p) Protein levels of E-cadherin, N-cadherin, vimentin in NCI-H460 cells transfected with in-miR-NC, in-miR-7-5p, in-miR-7-5p + si-con, or in-miR-7-5p + si-PFN2 and A549 cells transfected with miR-NC, miR-7-5p, miR-7-5p + pcDNA, or miR-7-5p + PFN2 were analyzed by WB. $^*p < 0.05$, $^{**}p < 0.01$, and $^{***}p < 0.001$
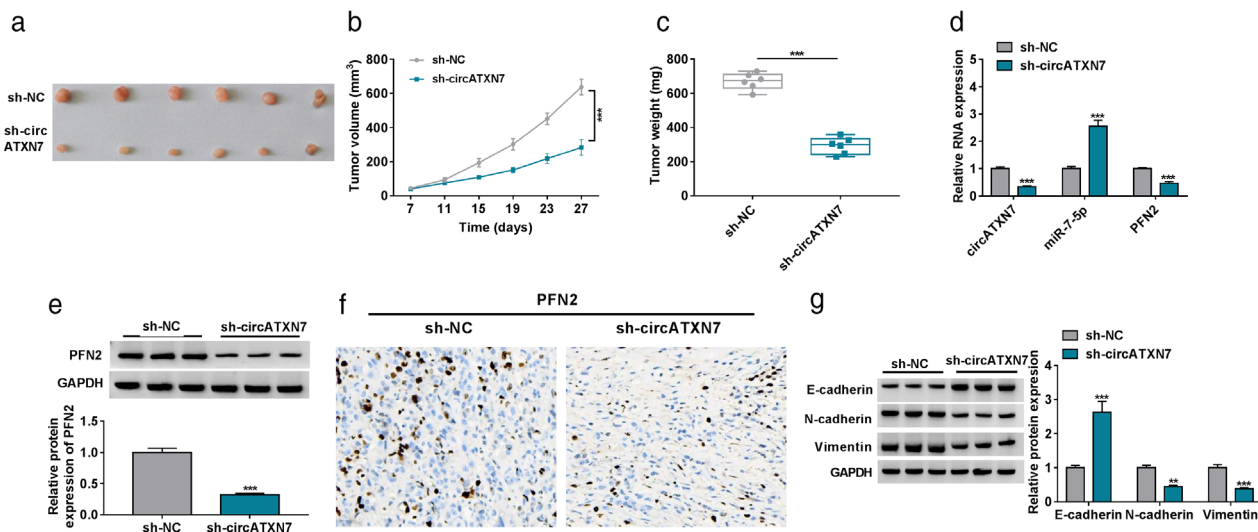
FIGURE 8 Inhibition of circATXN7 decreased NSCLC growth in vivo. (a) Representative images of xenograft tumors in sh-circATXN7 and sh-NC groups. (b) The growth curve of tumor volume in sh-circATXN7 and sh-NC groups. (c) The weight of xenograft tumors in sh-circATXN7 and sh-NC groups. (d) RT-qPCR assessed the expression of circATXN7, miR-7-5p, and PFN2 mRNA in xenograft tumors in sh-circATXN7 and sh-NC groups. (e and f) WB and IHC revealed the level of PFN2 protein in xenograft tumors in sh-circATXN7 and sh-NC groups. (g) WB analyzed protein levels of E-cadherin, N-cadherin, and vimentin in xenograft tumors in sh-circATXN7 and sh-NC groups. **$p < 0.01$ and ***$p < 0.001$
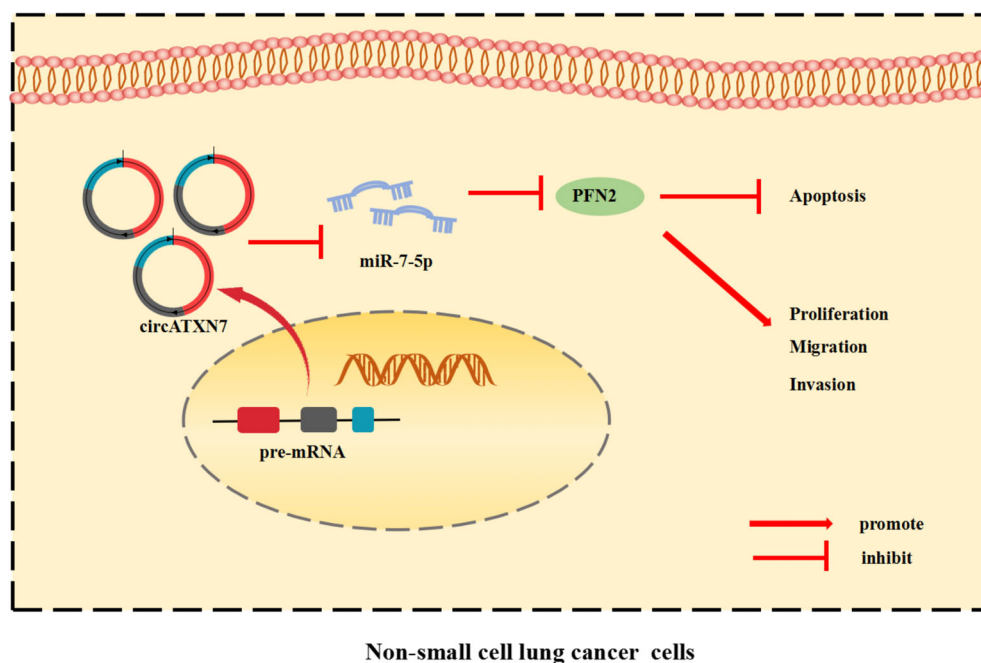
FIGURE 9 Schematic illustration showing the mechanism of circATXN7 promotes NSCLC malignant phenotypes

metastasis, invasion, and EMT in vitro, whereas circATXN7 overexpression exerted the opposing function; (3) circATXN7 silencing repressed NSCLC cell growth and EMT in xenograft mouse models. A previous study revealed that the parent gene ATXN7 of circATXN7 was an oncogene.[30] Moreover, circATXN7 could elevate ENTPD4 expression through functioning as an miR-4319 sponge, resulting in promoting GC cell growth and metastasis.[11] Also, hsa_circ_0007761 (hsa_circATXN7_007) had been exposed to be regulated in NSCLC, and hsa_circ_0007761 silencing curbed invasion and proliferation of NSCLC

cells.[31] Our results are consistent with these reports and offer evidence to support that circATXN7 exerts a promoting effect on NSCLC progression.

Recent studies have demonstrated that circRNAs can adsorb miRs through miR response elements to modulate gene expression, thus affecting the progression of NSCLC.[29] Thus, we verified circATXN7 as a miR-7-5p decoy. MiR-7-5p could repress Dox-induced homologous recombination repair via targeting PARP1, thus elevating the sensitivity of small cell LC cells to Dox.[17] In contrast, miR-7-5p targeted Bcl-2 and PARP1 to promote autophagy and decrease DNA

repair activity, thus maintaining energy homeostasis in cisplatin-resistant cervical cancer cells, and might be related to the cell-specific expression.[19] Herein, forced miR-7-5p expression overturned the promoting influence of circATXN7 upregulation on NSCLC cell malignant behaviors, whereas miR-7-5p inhibitor counteracted circATXN7 silencing-mediated repressive influence on NSCLC cell malignancy. These data illustrated that circATXN7 regulated NSCLC cell malignant behaviors through adsorbing miR-7-5p. Notably, miR-7-5p could repress NSCLC cell metastasis by targeting NOVA2.[20] Our data exhibited that circATXN7 over-expression elevated the NOVA2 protein level in NSCLC cells, but circATXN7 silencing reduced the NOVA2 protein level (Figure S1). These results manifested that circATXN7 might regulate NOVA2 expression by sequestering miR-7-5p. In the future, the relationship between NOVA2 and circATXN7 should be discussed in depth.

Accumulated studies have revealed that PFN2 upregulation is associated with the advancement of a variety of cancers. Researchers have found that PFN2 activated PI3K/AKT/β-catenin pathway, thus accelerating head and neck cancer cell metastasis and proliferation.[24] Also, hnRNPA2/B1 repressed breast cancer cell metastasis via binding PFN2 at least partly.[32] Moreover, PFN2 constrained the recruitment of HDAC1 to the Smad2 and Smad3 pro-moters, thus facilitating metastasis and growth of LC.[33] MiR-30a-5p targeted PFN2 to curb cell EMT in high inva-sive NSCLC.[25] Herein, PFN2 was verified as a miR-7-5p tar-get. Furthermore, PFN2 silencing restored miR-7-5p inhibitor-mediated promoting effect on NSCLC cell malig-nant behaviors, but PFN2 elevation offset the repressive impact of miR-7-5p mimic on NSCLC cell malignancy, manifesting that miR-7-5p constrained NSCLC cell malig-nancy through downregulating PFN2. Importantly, circATXN7 modulated PFN2 expression by adsorbing miR-7-5p in NSCLC cells. Thus, we concluded that circATXN7 promoted the growth of NSCLC via increasing PFN2 expression through sponging miR-7-5p.

In conclusion, circATXN7 exerted a promoting impact on NSCLC progression. Mechanically, circATXN7 adsorbed miR-7-5p to elevate PFN2 expression, thus promoting NSCLC cell proliferation, metastasis, invasion, and EMT (Figure 9). The study offered evidence to support the carci-nogenic effect of circATXN7 on NSCLC.

CONFLICT OF INTEREST

The authors declare that they have no conflicts of interest.

ORCID

Yongming Song https://orcid.org/0000-0003-1363-8444

REFERENCES

1. Siegel RL, Miller KD, Jemal A. Cancer statistics, 2020. CA Cancer J Clin. 2020;70:7–30.
2. Schwartz AG, Cote ML. Epidemiology of lung cancer. Adv Exp Med Biol. 2016;893:21–41.
3. Herbst RS, Morgensztern D, Boshoff C. The biology and management of non-small cell lung cancer. Nature. 2018;553:446–54.
4. Wadowska K, Bil-Lula I, Trembecki Ł, Śliwińska-Mossoń M. Genetic markers in lung cancer diagnosis: a review. Int J Mol Sci. 2020;21:4569.
5. Rajappa A, Banerjee S, Sharma V, Khandelia P. Circular RNAs: emerging role in cancer diagnostics and therapeutics. Front Mol Bio-sci. 2020;7:577938.
6. Cheng D, Wang J, Dong Z, Li X. Cancer-related circular RNA: diverse biological functions. Cancer Cell Int. 2021;21:11.
7. Chen LL. The expanding regulatory mechanisms and cellular func-tions of circular RNAs. Nat Rev Mol Cell Biol. 2020;21:475–90.
8. Drula R, Braicu C, Harangus A, Nabavi SM, Trif M, Slaby O, et al. Critical function of circular RNAs in lung cancer. Wiley Interdiscip Rev RNA. 2020;11:e1592.
9. Liang Y, Wang H, Chen B, Mao Q, Xia W, Zhang T, et al. circDCUN1D4 suppresses tumor metastasis and glycolysis in lung adenocarcinoma by stabilizing TXNIP expression. Mol Ther Nucleic Acids. 2021;23:355–68.
10. Lu M, Xiong H, Xia Z-K, Liu B, Wu F, Zhang HX, et al. circRACGAP1 promotes non-small cell lung cancer proliferation by regulating miR-144-5p/CDKL1 signaling pathway. Cancer Gene Ther. 2020;28:197–211.
11. Zhang Z, Wu H, Chen Z, Li G, Liu B. Circular RNA ATXN7 promotes the development of gastric cancer through sponging miR-4319 and regulating ENTPD4. Cancer Cell Int. 2020;20:25.
12. Liang Z-Z, Guo C, Zou M-M, Meng P, Zhang TT. circRNA-miRNA-mRNA regulatory network in human lung cancer: an update. Cancer Cell Int. 2020;20:173.
13. Krol J, Loedige I, Filipowicz W. The widespread regulation of micro-RNA biogenesis, function and decay. Nat Rev Genet. 2010;11:597–610.
14. Rupaimoole R, Slack FJ. MicroRNA therapeutics: towards a new era for the management of cancer and other diseases. Nat Rev Drug Discov. 2017;16:203–22.
15. Zhang X, Niu W, Mu M, Hu S, Niu C. Long non-coding RNA LPP-AS2 promotes glioma tumorigenesis via miR-7-5p/EGFR/PI3K/AKT/c-MYC feedback loop. J Exp Clin Cancer Res. 2020;39:196.
16. Zhong Q, Huang J, Wei J, Wu R. Circular RNA CDR1as sponges miR-7-5p to enhance E2F3 stability and promote the growth of naso-pharyngeal carcinoma. Cancer Cell Int. 2019;19:252.
17. Lai J, Yang H, Zhu Y, Ruan M, Huang Y, Zhang Q. MiR-7-5p-mediated downregulation of PARP1 impacts DNA homologous recombination repair and resistance to doxorubicin in small cell lung cancer. BMC Cancer. 2019;19:602.
18. Xiao H. MiR-7-5p suppresses tumor metastasis of non-small cell lung cancer by targeting NOVA2. BMC Cancer. 2019;24:60.
19. Yang F, Guo L, Cao Y, Li S, Li J, Liu M. MicroRNA-7-5p promotes cisplatin resistance of cervical cancer cells and modulation of cellular energy homeostasis by regulating the expression of the PARP-1 and BCL2 genes. Med Sci Monit. 2018;24:6506–16.
20. Xiao H. MiR-7-5p suppresses tumor metastasis of non-small cell lung cancer by targeting NOVA2. Cell Mol Biol Lett. 2019;24:60.
21. Li Y, Grenklo S, Higgins T, Karlsson R. The profilin:Actin complex localizes to sites of dynamic Actin polymerization at the leading edge of migrating cells and pathogen-induced actin tails. Eur J Cell Biol. 2008;87:893–904.
22. Pilo Boyl P, Di Nardo A, Mulle C, et al. Profilin2 contributes to synap-tic vesicle exocytosis, neuronal excitability, and novelty-seeking behav-ior. EMBO J. 2007;26:2991–3002.
23. Ling Y, Cao Q, Liu Y, Zhao J, Zhao Y, Li K, et al. Profilin 2 (PFN2) promotes the proliferation, migration, invasion and epithelial-to-mesenchymal transition of triple negative breast cancer cells. Breast Cancer. 2021;28:368–78.
24. Chen Z, Zhou K, Chen J, et al. Profilin 2 promotes proliferation and metastasis of head and neck cancer cells by regulating PI3K/AKT/β-catenin signaling pathway. Breast Cancer. 2019;27:1079–88.
25. Yan J, Ma C, Gao Y. MicroRNA-30a-5p suppresses epithelial-mesenchymal transition by targeting profilin-2 in high invasive non-small cell lung cancer cell lines. Oncol Rep. 2017;37:3146–54.

26. Livak KJ, Schmittgen TD. Analysis of relative gene expression data using real-time quantitative PCR and the 2(-Delta Delta C [T]) method. Methods. 2001;25:402–8.

27. Huang W, Yang Y, Wu J, Niu Y, Yao Y, Zhang J, et al. Circular RNA cESRP1 sensitises small cell lung cancer cells to chemotherapy by sponging miR-93-5p to inhibit TGF-β signalling. Cell Death Differ. 2020;27:1709–27.

28. Wu P, Mo Y, Peng M, Tang T, Zhong Y, Deng X, et al. Emerging role of tumor-related functional peptides encoded by lncRNA and circRNA. Mol Cancer. 2020;19:22.

29. Li C, Zhang L, Meng G, Wang Q, Lv X, Zhang J, et al. Circular RNAs: pivotal molecular regulators and novel diagnostic and prognostic biomarkers in non-small cell lung cancer. J Cancer Res Clin Oncol. 2019;145:2875–89.

30. Montero-Conde C, Leandro-Garcia LJ, Chen X, Oler G, Ruiz-Llorente S, Ryder M, et al. Transposon mutagenesis identifies chromatin modifiers cooperating with in thyroid tumorigenesis and detects as a cancer gene. Proc Natl Acad Sci USA. 2017;114:E4951–E60.

31. Huang Q, Wang S, Li X, Yang F, Feng C, Zhong K, et al. Circular RNA ATXN7 is upregulated in non-small cell lung cancer and promotes disease progression. Oncol Lett. 2019;17:4803–10.

32. Liu Y, Li H, Liu F, Gao LB, Han R, Chen C, et al. Heterogeneous nuclear ribonucleoprotein A2/B1 is a negative regulator of human breast cancer metastasis by maintaining the balance of multiple genes and pathways. EBioMedicine. 2020;51:102583.

33. Tang Y-N, Ding W-Q, Guo X-J, Yuan XW, Wang DM, Song JG. Epigenetic regulation of Smad2 and Smad3 by profilin-2 promotes lung cancer growth and metastasis. Nat Commun. 2015;6:8230.

SUPPORTING INFORMATION

Additional supporting information may be found in the online version of the article at the publisher's website.

How to cite this article: Li D, Fu Z, Dong C, Song Y. Downregulation of circATXN7 represses non-small cell lung cancer growth by releasing miR-7-5p. Thorac Cancer. 2022;13(11):1597–610. https://doi.org/10.1111/1759-7714.14426